Simulation of Hydrogen/Air Premixed Flames Propagating in a Spherical Vessel

By

Seishiro FUKUTANI and Hiroshi JINNO

(Received September 30, 1985)

Abstract

A mathematical model for an unsteady flame is established and applied to hydrogen/air premixed flames propagating spherically in a closed vessel. The model proposed in this investigation comprises the full reaction scheme for hydrogen combustion. It contains twenty-one elementary reactions and nine chemical species. The predicted burning velocities of hydrogen/air premixed flames with various combustion conditions are in good agreement with the experimental ones.

The linearity between the mass fraction of the burnt gas and the pressure proposed by Lewis and von Elbe is reproduced and verified to be valid, especially at the early stages of combustion. The reaction mechanism of hydrogen/air premixed flames propagating unsteadily is fairly similar to that of the steady flames. It can be divided into two parts, the low-temperature mechanism and the high-temperature mechanism. The boundary temperature is around 1000 K in all the flames. In a low-temperature region, the necessary amount of thermal energy to heat the combustible gas mixtures up to the boundary temperature is supplied in the form of chemical energy. It is transferred by the hydrogen atoms diffused from the flame fronts, and released mainly through the recombination reaction with oxygen.

1. Introduction

There are two types of premixed flames in general. They are the steady flames and the unsteady flames. For instance, a premixed flame stabilized on a burner belongs to the former group, and a flame developing in an internal combustion engine comes under the latter group.

An unsteady premixed flame propagating spherically is a fundamental model for flame propagation in an internal combustion engine and for an initial stage of detonation. A premixed flame of this type is also used to determine burning velocity as one of the most reliable methods. Andrews and Bradley have compared burning velocities of hydrogen/air premixed flames measured with a variety of experimental methods, the methods using steady flames and those using unsteady flames[1]. The

Department of Industrial Chemistry.

burning velocities measured by experiments, especially those obtained by means of the above two methods, do not necessarily agree with one another. Andrews and Bradley have further pointed out that there are some experimental errors caused by flame cooling on the burner edges in the steady-flame methods.

Several theoretical and experimental equations have been proposed for the evaluation of the burning velocity of a flame propagating in a spherical vessel[2-3]. Most of them are derived based only on thermodynamical relations such as an equation of state. They do not refer directly to the flame structure or to the propagation mechanism. The complicated interactions between chemical reactions and transport processes should inevitably be taken into account for any detailed analyses. One of the methods to avoid this difficulty is to apply computer simulation techniques to this problem.

The purpose of this investigation is to simulate unsteady hydrogen/air premixed flames propagating spherically by means of a mathematical model which includes a detailed reaction scheme, and to analyze their flame structure and propagation processes.

Bradley *et al.* have established a simple model, where chemical reactions are not taken into consideration explicitly, and have applied it to methane/air premixed flames[4]. Kooker has proposed a model for ozone/oxygen flames which have been assumed to include three elementary reactions[5]. He has reproduced some fundamental properties of these flames. He has also investigated the vibrational properties observed in the same flames[6]. Recently Kailasanath *et al.* have developed a model for hydrogen flames[7]. Their model includes a full chemical-reaction scheme for hydrogen/oxygen combustion. They have simulated the behavior of unsteady hydrogen flames at the initial stage, and predicted the minimum ignition energy and the quenching radius of these flames.

2. Mathematical Model

The following three assumptions were made for a mathematical model.

1. The flames contain OH, H, O, HO_2, H_2O_2, H_2O, H_2, O_2 and N_2; and twenty-one elementary reactions. (See Table 1.) Nitrogen is inert and works only as one of the third bodies in the recombination reactions.

2. The effects of viscosity and gravity are neglected. Radiative heat transfer inside a flame is also ignored.

3. Heat loss from a flame to vessel walls and heterogeneous reactions at the walls are not taken into consideration, that is, the vessel walls are adiabatic and inert.

These assumptions simplify the governing equations for unsteady flames. They are

Table 1. Hydrogen-Oxygen Reaction Scheme.

		$k=A \cdot T^n \cdot \exp(-E/T)$			
No.	Reaction	A	n	E	Ref
1.	$H_2+O_2 \longrightarrow OH+OH$	2.50E06	0.0	19600.0	8
2.	$H+O_2 \longrightarrow OH+O$	2.20E08	0.0	8450.0	8
3.	$O+H_2 \longrightarrow OH+H$	1.80E04	1.0	4480.0	8
4.	$OH+OH \longrightarrow O+H_2O$	6.30E06	0.0	550.0	8
5.	$OH+H_2 \longrightarrow H+H_2O$	2.20E07	0.0	2590.0	8
6.	$H+H+M \longrightarrow H_2+M$	2.60E06	−1.0	0.0	8
7.	$O+O+M \longrightarrow O_2+M$	1.90E01	0.0	−900.0	8
8.	$H+O+M \longrightarrow OH+M$	3.60E06	−1.0	0.0	9
9.	$OH+H+M \longrightarrow H_2O+M$	4.06E10	−2.0	0.0	8
10.	$H+O_2+M \longrightarrow HO_2+M$	5.00E03	0.0	−500.0	8
11.	$H+HO_2 \longrightarrow H_2+O_2$	2.50E07	0.0	350.0	8
12.	$H+HO_2 \longrightarrow OH+OH$	2.50E08	0.0	950.0	8
13.	$H+HO_2 \longrightarrow O+H_2O$	9.00E05	0.0	2000.0	8
14.	$OH+HO_2 \longrightarrow H_2O+O_2$	5.00E07	0.0	500.0	10
15.	$O+HO_2 \longrightarrow OH+O_2$	6.30E07	0.0	350.0	11
16.	$HO_2+H_2 \longrightarrow H+H_2O_2$	7.30E05	0.0	9400.0	8
17.	$HO_2+HO_2 \longrightarrow H_2O_2+O_2$	8.50E06	0.0	500.0	8
18.	$OH+H_2O_2 \longrightarrow HO_2+H_2O$	1.00E07	0.0	910.0	8
19.	$H+H_2O_2 \longrightarrow OH+H_2O$	2.20E09	0.0	5900.0	8
20.	$O+H_2O_2 \longrightarrow OH+HO_2$	2.80E07	0.0	3200.0	8
21.	$H_2O_2+M \longrightarrow OH+OH+M$	1.20E11	0.0	22900.0	8

k is expressed in m-mol-s units.

formulated as Eqs. (1) to (5) in the spherical coordinates.

$$\frac{\partial \rho}{\partial t}+\frac{1}{r^2}\frac{\partial}{\partial r}(r^2\rho v)=0 \tag{1}$$

$$\rho\frac{\partial v}{\partial t}+\rho v\frac{\partial v}{\partial r}=-\frac{\partial p}{\partial r} \tag{2}$$

$$\rho c_p\frac{\partial T}{\partial t}+\rho v c_p\frac{\partial T}{\partial r}=\frac{\partial p}{\partial t}+v\frac{\partial p}{\partial r}+\frac{1}{r^2}\frac{\partial}{\partial r}\left(r^2\lambda\frac{\partial T}{\partial r}\right)+\sum_i D_i\rho\frac{\partial \omega_i}{\partial r}\frac{\partial h_i}{\partial r}-\sum_i \phi_i h_i \tag{3}$$

$$\rho\frac{\partial \omega_i}{\partial t}+\rho v\frac{\partial \omega_i}{\partial r}=\frac{1}{r^2}\frac{\partial}{\partial r}\left(r^2 D_i\rho\frac{\partial \omega_i}{\partial r}\right)+\phi_i \tag{4}$$

$$p=\rho RT\sum_i\frac{\omega_i}{m_i} \tag{5}$$

where t denotes time; r, the radius; ρ, the density of a gas mixture; v, radial velocity; p, pressure; c_p, the specific heat; T, temperature; λ, the thermal conductivity; D, the diffusion coefficient; h, the enthalpy; ω, the mass fraction; ϕ, the

production rate due to chemical reactions; R, the universal gas constant; m, the molecular weight. The subscript i denotes the i-th species.

The rate constants of the reverse reactions were obtained on the basis of the equilibrium constants evaluated from JANAF data[12]. The binary diffusion coefficients and the thermal conductivities were estimated by using approximate equations[13].

The diameter of the vessel is 150 mm. The boundary conditions are such that the gradients of all the dependent variables are zero at the center, where a gas mixture is ignited, and at the walls of the vessel. In addition, the flow velocity is zero at the center and the walls. The initial pressure is atmospheric pressure. The ignition of unsteady flames in usually carried out by electric discharges in experiments. An ignition process by means of electric discharges is complicated and difficult to describe exactly because the discharges give a wide variety of effects to a combustible gas mixture depending on their strength and duration. Moreover, they actually bring a certain amount of enthalpy. However it is not yet well-known whether that enthalpy is given to the combustible gas mixture as thermal energy, or as chemical energy by producing active radicals or ions. The ignition energy is, therefore, simply assumed to be supplied only as thermal energy, and the initial distribution of temperature is given as a Gaussian distribution at the center of the vessel.

3. Results and Discussion

Figure 1 shows the velocity of a flame front relative to the gas flow, that is, the local burning velocity, or the socalled combustion velocity, of the three gas mixtures with the air ratios of 0.6, 1.0 and 1.667. The extrapolation of the curves

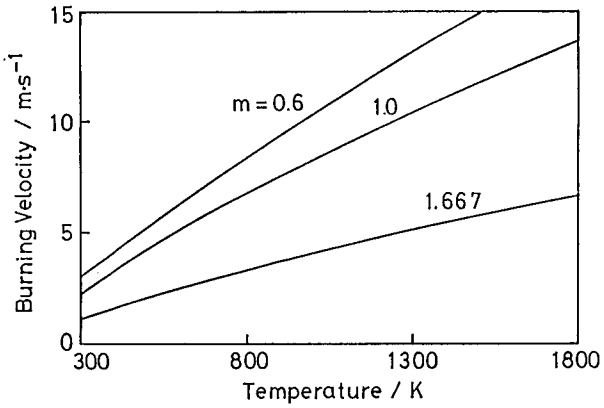

Fig. 1. Velocity of a flame front in the unsteady hydrogen flames with the air ratios of 0.6, 1.0 and 1.667.

to room temperature gives the burning velocity of the three flames due to the definition of the combustion velocity. The calculated values are 3.06 m/s for the flame with the air ratio of 0.6 (Hereafter, this combustion condition will, for instance, be simply denoted as $m=0.6$.), 2.28 m/s for the flame where $m=1.0$ and 1.10 m/s for $m=1.667$.

The mathematical model was verified by comparing the results predicted by means of the model with those obtained by the experiments using a spherical constant-volume vessel, which has the same diameter as that of the model. The comparison of these values with the ones obtained by the experiments is shown in Fig. 2. The calculated values agree well with the experimental ones. The burning velocity predicted by means of a mathematical model should be determined as a result of the overall contributions of the chemical and physical processes constituting the model. The good agreement permits us to conclude that this model can represent the combustion phenomena in actual hydrogen/air flames propagating unsteadily in a closed spherical vessel.

As described above, the measurement of burning velocity by means of unsteady premixed flames becomes popular because it can yield reliable data. Many expres-

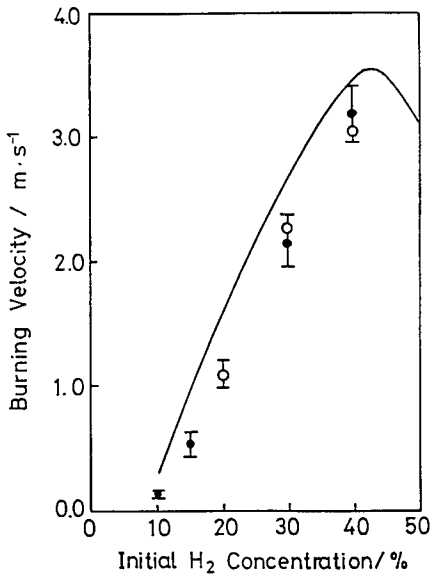

Fig. 2. Comparison of the burning velocities obtained by the simulation and the experiments. The open circles denote the calculated values in this study, and the closed circles are the values obtained with the coroesponding experiments. A solid line indicates the experimental values obtained by Andrews *et al*[14].

sions for the evaluation of burning velocity have been proposed on the basis of measured pressure and the position of a flame front. They have also been discussed from the standpoint of their validity and the range of their application. Lewis and von Elbe have given a relation that the pressure rise is proportional to the mass fraction of a burnt gas[15]. Their relation is useful and can simplify both measurement and calculation. The validity was examined using the mathematical model proposed here. The mass fraction of the burnt gas is plotted as a function of pressure in the three flames with the air ratios of 0.6, 1.0 and 1.667 in Fig. 3. The mass fraction increases linearly at least in a low-pressure region, when the flames extend up to more than 50 mm. Then, also in this investigation, their relation is ascertained to be valid.

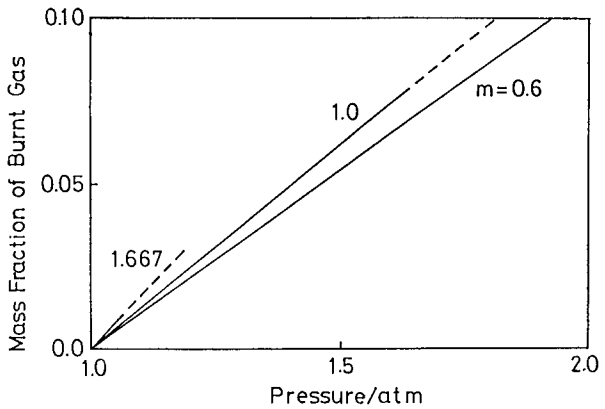

Fig. 3. Mass fraction of a burnt gas as functions of pressure in the hydrogen flames with the air ratios of 0.6, 1.0 and 1.667.

The three stoichiometric flames spreading up to 10 mm, 30 mm and 50 mm in the radius, and in addition, the two flames with the air ratios of 0.6 and 1.667 developing up to 10 mm will be investigated in the following. The instantaneous position of a flame front was defined to be the position of the maximum density gradient at that moment. This definition seems to be consistent with that in the experiments, where the flame position is usually measured by a schlieren method. The stoichiometric flame propagates to 10 mm at 0.61 ms after ignition, 30 mm at 1.71 ms and 50 mm at 2.84 ms. On the other hand, the rich and the lean flames ($m=0.6$ and 1.667) extend to 10 mm in the radius at 0.55 ms and 1.22 ms, respectively.

Figure 4 shows the temperature profiles of the stoichiometric flame every 0.2 ms including the initial profile. The radius of the flame front increases to 52 mm during

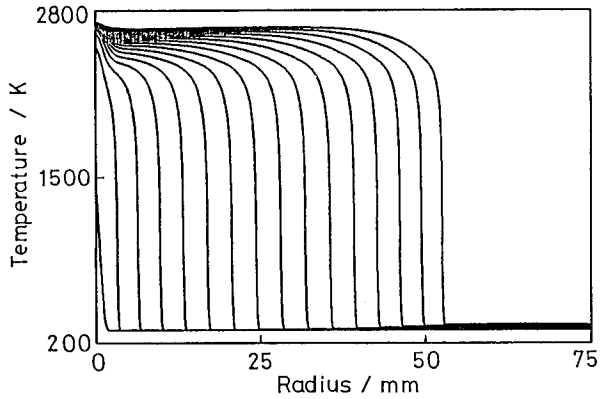

Fig. 4. Temperature profiles in the stoichiometric hydrogen flame every 0.2 ms and the initial profile.

3 ms after ignition, and the temperature of the unburnt gas is raised to 345 K due to adiabatic compression. The maximum temperature gradients are 4740 K/mm at 10 mm in the radius, 4870 K/mm at 30 mm and 5920 K/mm at 50 mm. These values are roughly comparable with that in the one-dimensional steady premixed flame with the same air ratio, 5480 K/mm. The position of the rich flame ($m=0.6$) is 1.2 times as large as that of the stoichiometric flame, and that of the lean flame ($m=1.667$) is about a half. The temperature gradients in the two nonstoichiometric flames are slightly smaller than those in the stoichiometric flames (0.92 and 0.93 times, respectively). The spatial distribution of pressure is very uniform and independent of the position of the flame and the gas composition. It does not show any drastic changes due to detonation.

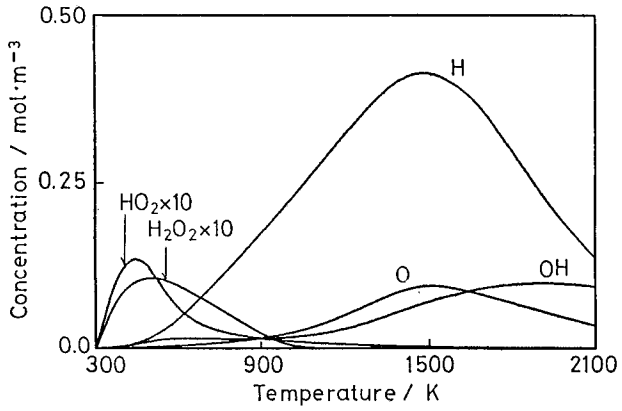

Fig. 5. Concentration profiles of the active species in the stoichiometric hydrogen flame with 10 mm in the radius.

Figure 5 depicts the concentration changes of the active species and the intermediates, which are expected to play an important role in the combustion reaction, in the stoichiometric flame with the radius of 10 mm. The concentrations of HO_2 and H_2O_2 have maxima at 440 K and 510 K, respectively, though they are small. This implies that some chemical reactions have already started even in such a low temperature region and even in the stoichiometric hydrogen flame propagating in a closed vessel. Hydroxyl radicals reveal the first small maximum in their concentration in a low temperature region and then the second maximum around 1900 K. This suggests also the beginning of chemical reactions at low temperatures.

One of the main objectives of flame propagation theories is to elucidate how the temperature is raised especially in a low-temperature region. The heat release due to chemical reactions makes the greatest contribution to the increase in the unsteady hydrogen/air flames among four terms appearing in the conservation equation of thermal energy, Eq. (3), that is, thermal conduction, heat transfer accompanying diffusion, compression-expansion and heat release due to reactions. (See Fig. 6.) Figure 7 shows the heat release rate in the various flames as functions of temperature. In all the flames, the heat release is observed even at temperatures as

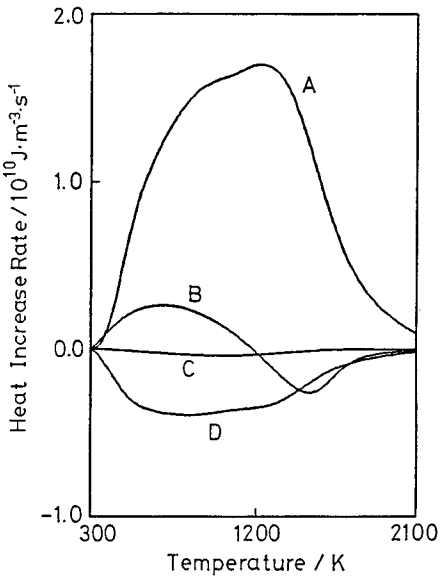

Fig. 6. Heat increase rates in the stoichiometric hydrogen flame with 10 mm in the radius.
A : heat release due to chemical reactions
B : thermal conduction
C : heat transfer accompanying diffusion
D : compression-expansion

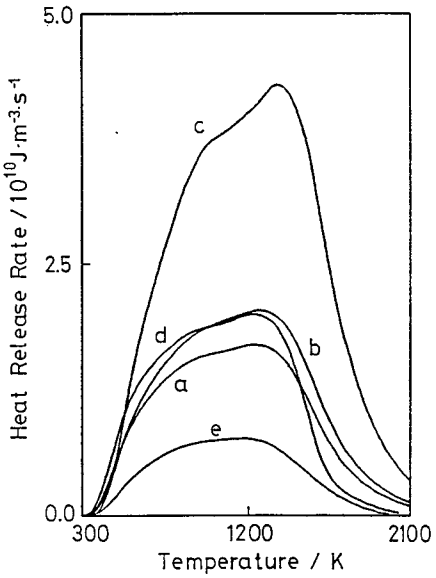

Fig. 7. Heat release rates due to chemical reactions.
a : m=1.0, r=10 mm b : m=1.0, r=30 mm
c : m=1.0, r=50 mm d : m=0.6, r=10 mm
e : m=1.667, r=10 mm

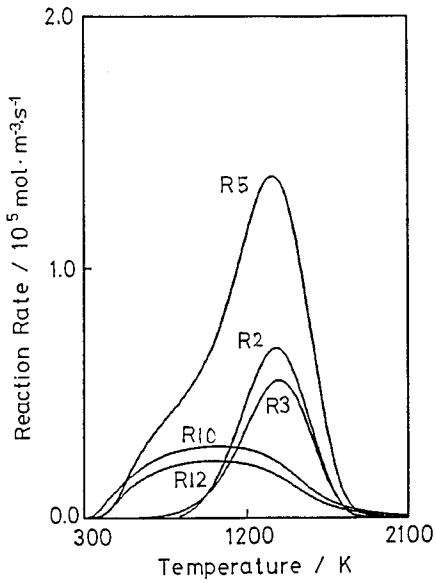

Fig. 8. Reaction rates in the stoichiometric hydrogen flame with 10 mm in the radius.
R2 : $H+O_2 \longrightarrow OH+O$ R3 : $O+H_2 \longrightarrow OH+H$
R5 : $OH+H_2 \longrightarrow H+H_2O$ R10 : $H+O_2+M \longrightarrow HO_2+M$
R12 : $H+HO_2 \longrightarrow OH+OH$

low as 600 K. Those rates increase steeply with an increasing temperature up to 900 K, and then slowly decrease after reaching a maximum at 1200-1400 K. It should be noted that the appreciable quantity of thermal energy is produced by chemical reactions even in a low-temperature region.

The reaction rate of five predominant chemical reactions in the stoichiometric flame with 10 mm in the radius is given in Fig. 8. As was previously pointed out with regard to the reaction mechanism in steady hydrogen flames, the following two reaction mechanisms can be distinguished clearly in all the unsteady hydrogen flames investigated in this work. The low-temperature mechanism was composed of reactions

$$H+O_2+M\longrightarrow HO_2+M \quad , \qquad (R10)$$

$$H+HO_2\longrightarrow OH+OH \quad , \qquad (R12)$$

$$OH+H_2\longrightarrow H+H_2O \quad ; \qquad (R5)$$

and the high-temperature mechanism was composed of reactions

$$H+O_2\longrightarrow OH+O \quad , \qquad (R2)$$

$$O+H_2\longrightarrow OH+H \qquad (R3)$$

and (R5).

The rates of reaction (R5) are plotted in Fig. 9 under the assumption that this

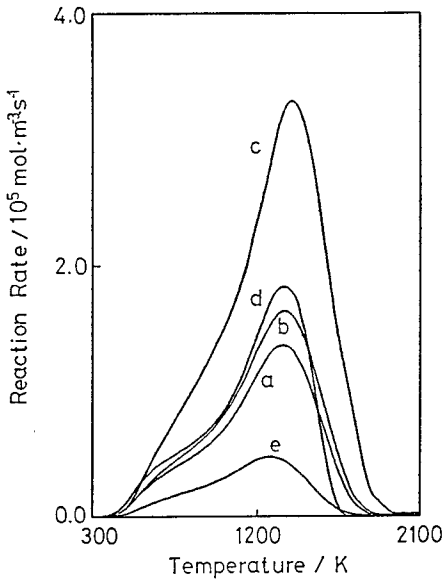

Fig. 9. Rates of reaction (R5), $OH+H_2\longrightarrow H+H_2O$.

a : $m=1.0$, $r=10$ mm
b : $m=1.0$, $r=30$ mm
c : $m=1.0$, $r=50$ mm
d : $m=0.6$, $r=10$ mm
e : $m=1.667$, $r=10$ mm

oxidation of hydrogen can be representative of the overall combustion reaction in these flames. Those rates change in conformity in all the flames.

Reactions (R10) and (R12) govern the heat release at temperatures lower than 1000 K. The contribution of reaction (R3), in addition to those of the two reactions, becomes important up to 1500 K. Then, recombination reactions (R10) and

$$H+OH+M \longrightarrow H_2O+M \qquad (R9)$$

are predominant in higher temperature regions.

Figure 10 presents the relation between the rate of reaction (R5) as the overall reaction and the rate of heat increase due to chemical reactions. These relations can distinguishably be divided into two parts. Moreover, the slopes observed in all the flames are approximately equal to one another in both regions. The gas temperature corresponding to the intersecting point is around 900 K in all the flames. This temperature represents the position in the flames where the high-temperature reaction mechanism takes place. (See Figs. 8 and 9.) The rate of reaction (R2) becomes equal to that of reaction (R10) at about 1000 K. The heat increase rates decrease around 900 K due to the endothermic effect of the two chain-branching reactions (R2) and (R3). The high-temperature mechanism, however, can prolife-

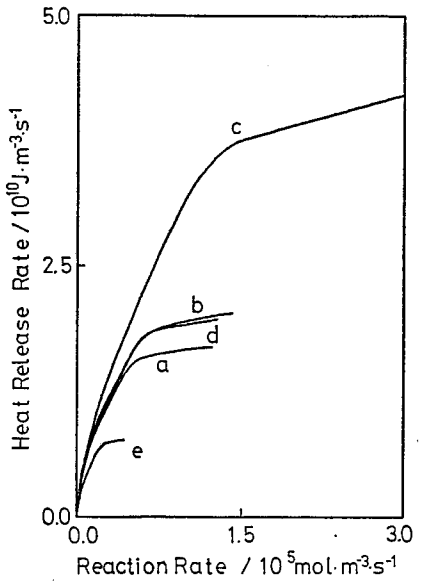

Fig. 10. Heat release rates as functions of the rate of reaction (R5), $OH+H_2 \longrightarrow H+H_2O$.

a : $m=1.0$, $r=10$ mm
b : $m=1.0$, $r=30$ mm
c : $m=1.0$, $r=50$ mm
d : $m=5.6$, $r=10$ mm
e : $m=1.667$, $r=10$ mm

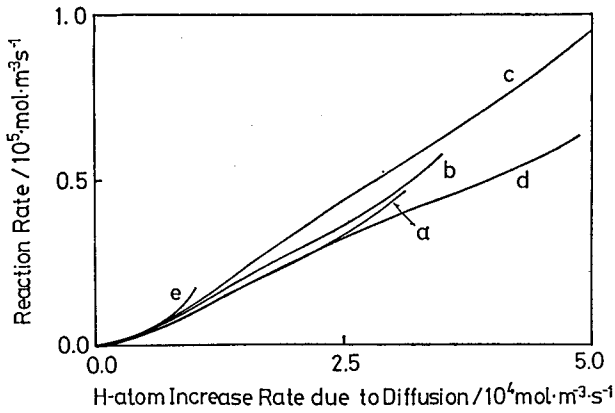

Ffg. 11. Rates of reaction (R5), $OH+H_2 \longrightarrow H+H_2O$, as functions of the rate of the increase in hydrogen atoms due to diffusion.

a : $m=1.0$, $r=10$ mm b : $m=1.0$, $r=30$ mm
c : $m=1.0$, $r=50$ mm d : $m=0.6$, $r=10$ mm
e : $m=1.667$, $r=10$ mm

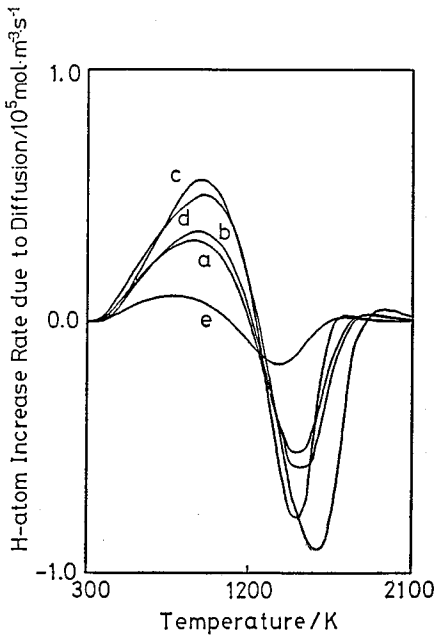

Fig. 12. Rates of the increase in hydrogens atom due to diffusion.

a : $m=1.0$, $r=10$ mm b : $m=1.0$, $r=30$ mm
c : $m=1.0$, $r=50$ mm d : $m=0.6$, $r=10$ mm
e : $m=1.667$, $r=10$ mm

rate hydrogen atoms and then the overall reaction rate increases exponentially until the hydrogen is exhausted. On the contrary, the low-temperature mechanism cannot proliferate them by itself. The increase in temperature in a low-temperature region does not result in an increase in the overall reaction rate, because the trigger reaction (R10) of the low-temperature mechanism has negative activation temperature. The excitation of the combustion reaction at low temperatures can be ascribed to the increase in the H-atom concentration due to diffusion. The rate of reaction (R5) is plotted as a function of the rates of the increase in hydrogen atoms due to diffusion, as shown in Fig. 11. All the flames give almost linear relations.

Figure 12 shows the increase rates of hydrogen atoms due to diffusion. Those rates increase almost linearly in the range of 400 K to 900 K, except for that in the lean flame. Even in a low-temperature region hydrogen atoms diffuse from a flame front. Enthalpy is, therefore, transferred into the low-temperature regions not as thermal energy but mainly as chemical energy in these flames. Diffusion of hydrogen atoms plays a very important role in unsteady hydrogen/air flames.

4. Concluding Remarks

The analyses of hydrogen/air premixed flames propagating unsteadily in a closed vessel by means of computer simulation give the following conclusions.

1. The mass fraction of a burnt gas is proportional to the fractional increase in pressure in a low-pressure region, and the expression of Lewis and von Elbe is valid in this pressure region.

2. The temperature increase in a low-temperature region can be ascribed to the heat release due to reactions. The chemical reactions, therefore, govern the propagation of unsteady hydrogen/air flames. The reactions in this region, and then the heat release, depend entirely upon the diffusion of hydrogen atoms.

References

1) G. E. Andrews and D. Bradley; Combust. Flame 18, 133 (1972).
2) K. H. O'Donovan and C. J. Rallis; Combust. Flame 3, 201 (1959).
3) S. P. Sharma, D. D. Agrawl and C. P. Gupta; Eighteenth Symposium (International) on Combustion, The Combustion Institute, Pittsburgh, p. 493 (1981).
4) D. Bradley and A. Mitcheson; Combust. Flame 26, 201 (1976).
5) D. E. Kooker; Seventeenth Symposium (International) on Combustion, The Combustion Institute, Pittsburgh, p. 1329 (1978).
6) D. E. Kooker; Combust. Flame 49, 141 (1983).
7) K. Kailasanath, E. Oran and J. Boris; Combust. Flame 47, 173 (1982).
8) D. L. Baulch, D. D. Drysdale, D. G. Horne and A. C. Lloyd; "Evaluated Kinetic Data for High Temperature Reactions", vol. 1, Butterworths, London (1972).
9) D. E. Jensen and G. A. Jones; Combust. Flame 32, 1 (1978).
10) M. P. Heap, T. J. Tyson, J. E. Cichanowicz, R. Gershman and C. J. Kau; Sixteenth

Symposium (International) on Combustion, The Combustion Institute, Pittsburgh, p. 535 (1976).
11) D. L. Baulch, D. D. Drysdale, J. Duxbury and S. Grant; "Evaluated Kinetic Data for High Temperature Reactions", vol. 3, Butterworths, London (1976).
12) D. R. Stull and H. Prophet; "JANAF Thermochemical Tables", 2nd ed., U. S. Dept. of Commerce, Washington (1971).
13) R. H. Perry and C. H. Chilton; "Chemical Engineers' Handbook", 5th ed., McGraw-Hill, New York (1973).
14) G. E. Andrews and D. Bradley; Combust. Flame 20, 77 (1973).
15) B. Lewis and G. von Elbe; "Combustion, Flames and Explosions of Gases", 2nd ed., Academic Press, New York (1961).